Value of aortic volumes assessed by automated segmentation of 3D MRI data in patients with thoracic aortic dilatation: A case-control study

Thomas Dietenbeck, Kevin Bouaou, Sophia Houriez-Gombaud-Saintonge, Jia Guo, Umit Gencer, Etienne Charpentier, Alain Giron, Alain de Cesare, Vincent Nguyen, Antonio Gallo, et al.

HAL Id: hal-04084103

https://hal.sorbonne-universite.fr/hal-04084103

Submitted on 27 Apr 2023

Value of aortic volumes assessed by automated segmentation of 3D MRI data in patients with thoracic aortic dilatation: a case–control study

Thomas Dietenbeck[a,b§], Kevin Bouaou[a,b], Sophia Houriez--Gombaud-Saintonge[a,b,c], Jia Guo[a,b], Umit Gencer[d,e], Etienne Charpentier[a,b,f], Alain Giron[a], Alain De Cesare[a], Vincent Nguyen[a,b], Antonio Gallo[a,b], Samia Boussouar[f], Nicoletta Pasi[f], Gilles Soulat[d,e], Alban Redheuil[a,b,f], Elie Mousseaux[d,e], Nadjia Kachenoura[a,b]

[a]Sorbonne Université, CNRS, INSERM, Laboratoire d'Imagerie Biomédicale, LIB, F-75006 Paris, France
[b]Institute of Cardiometabolism and Nutrition (ICAN), F-75013 Paris, France
[c]ESME Sudria Research Lab, F-75006 Paris, France
[d]Université de Paris, PARCC, INSERM, F-75015 Paris, France
[e]Assistance Publique Hôpitaux de Paris, Hôpital Européen Georges Pompidou, F-75015 Paris, France
[f]Imagerie Cardio-Thoracique (ICT), Sorbonne Université, AP-HP, Groupe Hospitalier Pitié-Salpêtrière, F-75013 Paris, France.

Address for correspondence (§)

Thomas DIETENBECK (thomas.dietenbeck@sorbonne-universite.fr)
Laboratoire d'Imagerie Biomédicale,
Campus des Cordeliers, Escalier A - 4ème étage
15 rue de l'Ecole de Médecine, 75006 PARIS (France)
Phone: +33 1 44 27 91 19

Abstract

Purpose

The purpose of this study was to investigate the added value of aortic volumes compared to diameters or cross-sectional areas in separating patients with dilated aorta from matched controls.

Materials and Methods

Patients with tricuspid aortic valve and ATAA (TAV-ATAA: n=62, 15 women, median age 66 (60;75)[33-86] years) and patients with bicuspid aortic valve and dilated ascending aorta (BAV: n=43, 8 women, 51 (39;66)[17-76] years) were studied. Two control groups were matched by age and sex to TAV-ATAA (n=54, 15 women, 68 (59;73)[33-81] years) and BAV (n=42, 8 women, 50 (40;66)[17-77] years). All participants underwent 3D-MRI, used for 3D-segmentation for measuring aortic length, maximal diameter, maximal cross-sectional area (CSA) and volume for the ascending aorta (AAo).

Results

An increase in AAo volume (TAV-ATAA: +107%; BAV: +171% vs. controls, $P<0.001$) was found, which was 3 times higher than the increase in diameter (TAV-ATAA: +29%; BAV: +40% vs controls, $P<0.001$). Indexed aortic length, maximal diameter and CSA showed lower performance than volume (area under ROC curve [AUC], accuracy(%)=0.935 (0.882-0.989), 88.7 (82.9-94.5) for TAV-ATAA; 0.908 (0.829-0.987), 88.0 (80.9-95.0) for BAV vs. controls) in differentiating patients from their matched controls (AUC, accuracy(%), P-value for ROC comparisons against volume for TAV-ATAA: length=0.820(0.739-0.901), 78.3(70.7-85.8), <0.001, maximal diameter=0.867(0.795-0.939), 80.9(73.7-88.1), 0.003, CSA=0.900(0.836-0.964), 82.6(75.7-89.5), 0.03; BAV: length=0.827(0.730-0.924), 78.3(69.4-87.2), 0.02, maximal diameter=0.876(0.789-0.963), 83.1(75.1-91.2), 0.07, CSA=0.900(0.819-0.981), 86.8(79.5-94.0), 0.27).

Conclusions

Aortic volume measured by 3D-MRI integrates both elongation and luminal dilation, resulting in greater classification performance than maximal diameter and length in differentiating patients with dilated AAo or aneurysm from controls.

1. Background

Aortic dissection is a life-threatening condition that remains an unpredictable complication of aortic aneurysm, a mostly silent and progressive disease. The only aortic morphological measurement established as predictor of dissection in existing guidelines is the maximal aortic diameter and its growth rate [1]. However, in more than 50% of patients who ultimately experienced aortic dissection, the aortic diameter was found below the recommended surgical threshold [2].

Recent studies based on computed tomography (CT) have shown that in addition to significant aortic luminal dilation, patients with ascending thoracic aortic aneurysm (ATAA) also presented a significant elongation of the aorta [3,4]. The studies indicated that length and diameters were predictors of dissection independent of conventional risk factors [4], which suggests the need for multifactorial risk scores encompassing the most significant aortic morphological changes. Furthermore, both cohort [5–7] and computational fluid simulation [8] studies highlighted increased risk of aortic dissection with an increase in angle between the aortic root and brachiocephalic artery planes, induced by aortic tortuosity. Also, volume growth can occur in abdominal aortic aneurysm even though the maximal diameter remains stable [9] or in the ascending aorta of patients with descending aortic dissection and normal maximal diameters [10]. Thus, authors reported a higher reproducibility of aortic volume and its superiority for detecting aneurysm growth as compared with maximal diameters measured on selected slices [9,11].

Because repeated scans are often required for standard follow-up of patients with aortic disease, aortic MRI with continuously improving image quality and spatial resolution has emerged as an effective radiation-free modality for the 3D evaluation of aortic morphology [12]. Accordingly, the objective of this study was to investigate the added value of aortic volumes compared to diameters or cross-sectional areas in separating patients with dilated aorta from matched controls using a semi-automated segmentation [13] of 3D MRI images.

2. Methods

2.1. Study population

Patients with a tricuspid aortic valve and ascending thoracic aortic aneurysm (TAV-ATAA, n = 62, 15 women, median age 66 years (Q1; Q3 60; 75), [range 33-86]) and patients with a bicuspid aortic valve and dilated ascending aorta (BAV, n = 43, 8 women, median age 51 years (39; 66) [17-76]) and who underwent an aortic MRI between 2014 and 2018 were retrospectively included. ATAA was defined by a maximal diameter of the ascending aorta ≥ 41 mm or ≥ 22 mm/m² when indexed to body surface area (BSA). Exclusion criteria were concomitant presence of aortic valve stenosis, regurgitation graded more than moderate, aortic coarctation, Marfan or Turner syndrome, history of aortic dissection and previous surgery. Aortic valve function as well as BAV confirmation and fusion pattern were evaluated by using conventionally acquired stacks of 2D cine anatomical and velocity images perpendicular to the aortic root.

Controls were matched to TAV-ATAA patients (Ct, n = 54, 15 women, median age 68 years (59; 73) [33-81]) and BAV patients (Cb, n = 42, 8 women, median age 50 years (40; 66) [17-77]) by sex and age (±5 years). Of note, some of the controls (N=20) are both in the Ct and Cb groups. Controls were free of symptomatic cardiovascular disease, diabetes mellitus, dyslipidemia, renal disease, known inflammatory conditions and malignancy, but they could have treatment for hypertension (25/54 in the Ct group, 4/42 in the Cb group). We excluded controls with aortopathies, cardiomyopathies or valvular diseases revealed by MRI.

Age, sex, height, weight, BSA, body-mass index (BMI) and smoking status were collected immediately before the MRI acquisition. All study participants gave their informed consent, and the study protocol was approved by the local ethics committee (NCT03895541, NCT02701855, NCT03474159, NCT02517944). Figure 1 shows the study flow chart.

2.2. MRI protocol

All participants underwent MRI on a 3T magnet system (site 1: Discovery MR750w, GE Healthcare, Chicago; site 2: Prisma, Siemens Healthineers, Erlangen) or a 1.5T magnet system (site 3: Aera, Siemens Healthineers, Erlangen). Of note, sites 1 and 3 included both controls and patients, while site 2 included only controls. For sites 1 and 3, gadolinium-based contrast agent (Multihance, Bracco Imaging or Dotarem, Guerbet) was typically injected (0.1 to 0.2 mmol/kg) during the cardiovascular MRI examination for myocardial tissue characterization and thus prior to aortic acquisitions. For all sites, 3D data were acquired in a sagittal oblique volume encompassing the thoracic aorta during free breathing with electrocardiographic (diastasis) and respiratory (expiration) gating and with the following typical scan parameters: (site 1) spoiled gradient echo (SPGR), voxel size = $0.67 \times 0.67 \times 3.19$ mm³, echo time = 1.3 ms, repetition time = 3.1 ms and flip angle = 24°; (site 2) steady state free precession (SSFP), voxel size = $0.98 \times 0.98 \times 1$ mm³, echo time = 1.3 ms, repetition time = 311 ms and flip angle = 19°;

and (site 3) SSFP, voxel size = 0.66×0.66×1.13 mm^3, echo time = 1.5 ms, repetition time = 283 ms and flip angle = 90°.

Central blood pressure was recorded by using the SphygmoCor Xcel device (ATCOR Medical, Sydney [14]) simultaneously with MRI aortic acquisitions at all sites. Three measurements were recorded and their average provided central systolic blood pressure (cSBP) and diastolic blood pressure (cDBP) as well as pulse pressure (cPP), which was calculated as the difference between cSBP and cDBP.

2.3. Assessment of aortic morphology

The aorta was segmented by using a previously described custom-developed software (Mimosa, Sorbonne Université [13]) which was previously shown to be reproducible [13], and then used to establish normal values and age-related changes in thoracic aorta geometry [15]. Briefly, six anatomical landmarks were manually placed by an experienced operator (5 years) from the sino-tubular junction to the diaphragm and used to initialize the aortic centreline and delimit aortic segments. The aortic lumen was then automatically segmented by using a 3D active contour [16], and a final centreline was calculated. Finally, the segmented aorta was divided into 3 segments according to the European Society of Cardiology guidelines [17] by using the given landmarks (Fig. 1): the ascending aorta (AAo), defined as the segment between the sino-tubular junction and the brachiocephalic trunk; the aortic arch, defined as the segment comprising the supra-aortic arteries; and the descending thoracic aorta (DAo), defined as the segment between the left subclavian artery and the diaphragm.

For each aortic segment, 6 morphological indices were calculated: the centreline length, maximal diameter, maximal cross-sectional area (CSA), volume, total curvature [18,19] and tortuosity. Tortuosity was computed as $\frac{L_s - L_d}{L_d}$, where L_s is the true segment length along the centreline and L_d is the direct length between the segment extremities.

Total curvature was calculated as $\frac{1}{L_s} \int_0^{L_s} \frac{\|\dot{s} \wedge \ddot{s}\|}{\|\dot{s}\|^3} \, ds$, where s represents the 3D coordinates of the centreline and $\dot{s}$ and $\ddot{s}$ are the first and second derivatives of s, respectively. Total curvature was normalized by L_s to account for segment length [19].

2.4. Statistical analysis

All measurements are provided as median, interquartile range and minimal-maximal values [20,21] because some measurement distributions were not normal according to a Shapiro-Wilk normality test. Non-parametric Wilcoxon and chi-squared tests were used for comparing continuous and categorical variables, respectively, between patients and their matched controls on all aortic segments to study the extend of aortic morphological changes in dilated or aneurysmal patients. P < 0.05 was considered statistically significant. For all aortic indices, changes between patients and controls were reported as the percentage difference between their median values.

Receiver operating characteristic (ROC) curves were computed for each morphological parameter of the ascending aorta after indexation to BSA [22], and area under the ROC curve (AUC), accuracy, sensitivity and specificity were used along with the 95%

confidence intervals (CIs) to evaluate the ability of aortic indices to differentiate patients and their matched controls. ROC statistics were also estimated for aortic volumes without and with indexation to patient height [23] to evaluate the effect of different indexation strategies (BSA, height) on aortic volume classification performance. Cutoff values were identified on the ROC curve by using the Youden index, and the non-parametric test of DeLong [24] was used for comparing ROC curves. Aortic quantitative measures reproducibility was evaluated on 20 subjects randomly selected amongst all groups (5 datasets in each group). Aortic segmentation was performed by 2 users (TD, JG) and TD repeated the analysis 2 weeks later. The inter-observer and intra-observer variabilities were assessed using the coefficient of variation, calculated as the standard deviation of the differences between two measurements divided by their mean.

3. Results

The whole 3D segmentation process, including the loading of the data and the recording of the results, took less than 5 min per participant. Figure 2 shows examples of 3D aortic shapes corresponding to a healthy control, a TAV-ATAA patient and a BAV patient. The 3 illustrated aortas belong to men with similar age, height and BSA to more specifically illustrate aortic morphological changes.

3.1. Participant characteristics

Basic characteristics and blood pressure values are summarized in Table 1 for TAV-ATAA and BAV patients (N= 62 and 43, respectively) and their matched controls (N=54 and 42, respectively). Both TAV-ATAA and BAV groups were predominantly male, and BAV patients were younger than TAV-ATAA patients. BAV and matched controls did not differ in BSA ($P = 0.088$), BMI ($P = 0.539$) or blood pressure (cSBP: $P = 0.176$; cDBP: $P = 0.643$; cPP: $P = 0.585$), while BSA ($P = 0.023$) and cSBP ($P = 0.014$) were higher in the TAV-ATAA group as compared to their matched controls.

3.2. Morphological indices in TAV-ATAA patients

Morphological aortic indices of TAV-ATAA patients and their matched controls are shown in Table 2 and illustrated in Figure 3 for the 3 aortic segments: AAo, arch and DAo. The AAo diameter was significantly higher in TAV-ATAA patients than controls (difference between median values: maximal diameter: +9.17 mm, +29%, $P < 0.001$; maximal CSA: +7.57 cm^2, +68%, $P < 0.001$). This luminal dilation was concomitant with a significantly higher AAo length (+17.8 mm, +30%, $P < 0.001$), thus resulting in an overall significantly higher aortic volume (+43.9 mL, +107%, $P < 0.001$) in TAV-ATAA patients than their controls. Furthermore, the AAo curvature was significantly lower in TAV-ATAA patients than their controls (-0.0077 mm^{-1}, -22%, $P < 0.001$).
In addition to these changes in AAo morphology, TAV-ATAA patients and their controls showed differences in the aortic arch and DAo segments but to a lesser extent. Indeed, as compared with the control aortic arch, the aortic arch of TAV-ATAA patients had greater maximal diameter (+4.34 mm, +14%, $P < 0.001$), maximal CSA (+3.63 cm^2, +34%, $P < 0.001$) and volume (+9.18 mL, +40%, $P < 0.001$) as well as decreased curvature (-0.003 mm^{-1}, -11%, $P = 0.012$), but the length was similar (+1.4 mm, +4%, $P = 0.229$). Also, TAV-ATAA patients showed significantly greater DAo length (+20.7 mm, +13%, $P < 0.001$), maximal diameter (+3.31 mm, +13%, $P < 0.001$), maximal CSA (+2.1cm^2, +28%, $P < 0.001$) and volume (+27.1 mL, +38%, $P < 0.001$).

3.3. Morphological indices in BAV patients

The right part of Table 2 and Figure 4 present the aortic morphological indices for BAV patients and their controls. As compared with the control AAo, the AAo of BAV patients had significantly greater length (+21.3 mm, +39%, $P < 0.001$), maximal diameter (+12.0 mm, +40%, $P < 0.001$), and maximal CSA (+8.9 cm^2, +88%, $P < 0.001$), thus resulting in greater volume (+56.8 mL, +171%, $P < 0.001$). Also, BAV patients showed significantly lower AAo curvature (-0.0071 mm^{-1}, -19%, $P < 0.001$) and greater tortuosity (+0.051, +47%, $P = 0.0013$).

As compared with the control aortic arch, the aortic arch of BAV patients had significantly greater length (+5.80 mm, +17%, P = 0.013), maximal diameter (+5.77 mm, +20%, P < 0.001), maximal CSA (+4.0 cm^2, +41%, P < 0.001) and volume (+7.90 mL, +43%, P < 0.001). Also, BAV patients showed significantly greater DAo length (+13.3 mm, +8%, P = 0.010), maximal diameter (+1.80 mm, +8%, P = 0.036) and volume (+18.1 mL, +31%, P = 0.01).

3.4. ROC analysis

Table 3 reports the AUC, accuracy, sensitivity and specificity of the ROC analyses evaluating the ability of AAo length, maximal diameter, maximal CSA or volume, all indexed to BSA, to differentiate patients and their matched controls. In differentiating TAV-ATAA patients from their controls, the indexed AAo volume showed significantly higher performance (AUC / accuracy = 0.935 (0.882-0.989) / 88.7 (82.9-94.5)) than the remaining morphological indices (AUC / accuracy / p-value for ROC comparison against volume, 0.820 (0.739-0.901) / 0.79 (70.7-85.8) / < 0.001 for length, 0.867 / 0.809 / 0.003 for maximal diameter, 0.900 (0.882-0.989) / 0.826 (75.7-89.5) / 0.03 for maximal CSA).

In differentiating BAV patients from their matched controls, indexed AAo volume performance (AUC / accuracy = 0.908 (0.829-0.987) / 88.0 (80.9-95.0)) was higher in comparison to indexed AAo length (AUC / accuracy / P-value for ROC comparisons against volume = 0.827 (0.730-0.924) / 78.3 (69.4-92.6) / 0.02) and similar to indexed AAo maximal diameter or CSA (0.876 (0.789-0.963) / 83.1 (75.1-91.2) / 0.07 for maximal diameter, 0.900 (0.819-0.981) / 86.8 (79.5-94.0) / 0.27 for maximal CSA).

Classification performance for volume was stable independent of the indexation strategy for both TAV-ATAA and BAV versus their controls, with no statistically significant differences in AUC for both TAV-ATAA (AUC with no indexation = 0.942 (0.895 - 0.988), AUC with indexation to BSA = 0.935 (0.882 - 0.989), AUC with indexation to height = 0.942 (0.891 - 0.994); P-value no indexation vs BSA / height vs BSA indexed P = 0.12 / 0.16) and BAV (AUC with no indexation = 0.903 (0.836 – 0.971), AUC with indexation to BSA = 0.908 (0.829 - 0.987), AUC with indexation to height = 0.904 (0.823 – 0.984); P = 0.09 / 0.26).

3.5. Reproducibility study

In the AAo, the coefficient of variation (CoV) for the inter-observer (intra-observer) study was 10.8 % (6.8%) for the length, 2.6% (3.2%) for the maximal diameter, 5.6% (6.8%) for the maximal CSA and 10.9% (10.7%) for the volume. In the DAo, the CoV was 4.1 % (2.9%) for the length, 3.3% (3.7%) for the maximal diameter, 6.4% (7.5%) for the maximal CSA and 7.5% (8.8%) for the volume.

4. Discussion

This study used an automated 3D aortic segmentation method [13,15] for a comprehensive and reproducible morphological analysis of the thoracic aorta and its segments from 3D MRI images of patients with ascending thoracic aorta dilation and a tricuspid or bicuspid aortic valve. Ascending aortic volume indexed to BSA achieved higher AUC and accuracy than ascending aortic length, maximal luminal diameter and CSA in differentiating patients with dilated ascending aorta and a tricuspid or bicuspid aortic valve from age- and sex-matched controls. Finally, whether indexed to individuals' BSA and height or not, ascending aortic volume classification performance remained stable for both patient groups with a tricuspid or bicuspid valve.

The indexation of morphological cardiovascular indices to body size parameters has been widely debated in the literature [2,22,23]. Hence, the ability of the ascending aortic volume to differentiate patients with dilated ascending aorta and a tricuspid or bicuspid aortic valve from their controls was studied while evaluating the effect of indexation to body size. Regardless of the indexation strategy, similar AUC and accuracy for ascending aortic volume was found for both comparisons: TAV-ATAA and BAV versus their controls.

Aortic volume estimation has 2 original features because it integrates both aortic elongation and luminal dilation and its calculation is fully independent of slice positioning and obliqueness [25]. With the integration of both dilation and elongation in volume estimation, the change in volume in patients with aortic dilation was 3 times higher than changes in length and maximal diameter. The associated ROC analysis suggested that a better classification of patients with aortic dilation could be achieved by using volume versus length or maximal diameter. Furthermore, the reported semi-automated 3D segmentation provides robust estimates of maximal diameters perpendicular to the aortic centreline in any desired aortic segment along with segmental and global aortic length, tortuosity and curvature. These parameters in our patients with thoracic aorta dilatation varied in line with literature findings [3–7]. Finally, such 3D segmentation has been successfully transposed to the 4D flow MRI peak systolic modulus [26,27], thus resulting in hemodynamic aortic parameters. A combined use of aortic volumes along with the widely known maximal diameters and the newly proposed 4D flow parameters may enrich the MRI stratification capacities in various aortopathies [28,29].

The prevalence of hypertension considerably increases with age [30], so enrolling older healthy individuals without cardiovascular comorbidities was difficult. Accordingly, individuals with controlled hypertension were included in our control groups, especially controls for TAV-ATAA patients, to ensure age matching with patients. However, this inclusion did not change the relevance of the head-to-head comparison of the various aortic morphological indices in differentiating patients with thoracic aorta dilatation from controls. Indeed, because hypertensive patients usually exhibit subclinical aortic luminal dilation and elongation [15], their inclusion would only increase the overlap between patients and controls and thus potentially limit the classification performance of all tested aortic morphological indices.

This study included data from 3 different centers with acquisitions performed at 1.5T or 3T. Though the sample size and age imbalance did not allow for comparison between centers or magnets, one might note that all subjects were successfully segmented using our software irrespective of the acquisition site, injection protocol or magnetic field strength. This observation highlights the ability of MRI to accurately quantify aortic morphology which is of particular interest, since MRI is the recommended modality for the follow-up of aortic disease in younger patients [31]. Such capacities combined with ongoing research in MRI to accelerate sequences, saturate fat components and improve spatial resolution for the 3D MRI aortic sequences as well as automated 3D image processing tools will ultimately enhance the recommendation of MRI in aneurysmal patients follow-up and managements.

The main limitation of this study is its cross-sectional design. Longitudinal data and patient outcomes would have been of major interest to study 1) the growth rate of the studied morphological parameters and 2) the relation between these parameters and outcomes of patients. The exclusion of the aortic root is another limitation of this study because ascending aortic dilatation may occur in this segment. Of note, because of the complex shape of the sinus of Valsalva, especially in patients with a very proximal aneurysm, the sinus of Valsalva was not included in the semi-automated segmentation. This exclusion may explain the maximal diameters below the aneurysmal threshold in the patient groups. However, the rationale of this study was to compare the ability of morphological parameters to separate patients with aneurysm from healthy controls according to the same aortic segment. A possible way of measuring the sinus of Valsalva could be by a dedicated sequence following the protocol described in [32,33] that would allow using 2D automatic segmentation tools [34,35] or by the use 3D MRI sequence centered on the heart to segment the sinus of Valsalva while combining active contours and shape priors [36].

5. Conclusions

This paper describes a semi-automated 3D MRI quantification of morphological changes in the thoracic aorta, comparing patients with dilated ascending aorta and a tricuspid or bicuspid aortic valve with their matched controls. In addition to the expected luminal dilation of the ascending aorta, a significantly greater ascending aortic length along with an increase in volume were observed in patients with aneurysm versus their age- and sex-matched controls. The ascending aortic volume was able to discriminate patients with aneurysm based on the established definition from controls, with higher accuracy than other aortic morphological indices. The performance of the aortic volume in separating patients from controls remained stable regardless of body size indexation.

Authors' contributions

AR, EM, NK and TD designed the study. AGa, AR, EC, EM, GS, NP, SB carried out the data acquisition. EC, JG, KB, SHGS, TD, VN and UG carried out the experiments and technical developments. AGi, AR, EM, NK and TD interpreted the results. NK and TD drafted the manuscript. All authors edited and revised the manuscript. All authors read and approved the final version of the manuscript.

Informed consent and patient details

The authors declare that this report does not contain any personal information that could lead to the identification of the patients.

Availability of data and materials

The datasets used and/or analyzed during the current study are available from the corresponding author on reasonable request.

Competing interests

The authors declare that they have no competing interests

References

[1] Evangelista A, Isselbacher EM, Bossone E, Gleason TG, DiEusanio M, Sechtem U, et al. Insights from the International Registry of Acute Aortic Dissection: a 20-year experience of collaborative clinical research. Circulation 2018;137:1846--1860.

[2] Pape LA, Tsai TT, Isselbacher EM, Oh JK, O'Gara PT, Evangelista A, et al. Aortic diameter >= 5.5 cm is not a good predictor of Type A aortic dissection observations from the International Registry of Acute Aortic Dissection (IRAD). Circulation 2007;116:1120–7.

[3] Krüger T, Forkavets O, Veseli K, Lausberg H, Vöhringer L, Schneider W, et al. Ascending aortic elongation and the risk of dissection. Eur J Cardiothorac Surg 2016.

[4] Heuts S, Adriaans BP, Gerretsen S, Natour E, Vos R, Cheriex EC, et al. Aortic elongation part II: the risk of acute type A aortic dissection. Heart 2018;104:1778--1782.

[5] Gode S, Akinci O, Ustunısık CT, Sen O, Kadirogulları E, Aksu T, et al. The role of the angle of the ascending aortic curvature on the development of type A aortic dissection: ascending aortic angulation and dissection. Interact Cardiovasc Thorac Surg 2019;29:615--620.

[6] Alhafez BA, Truong VTT, Ocazionez D, Sohrabi S, Sandhu H, Estrera A, et al. Aortic arch tortuosity, a novel biomarker for thoracic aortic disease, is increased in adults with bicuspid aortic valve. Int J Cardiol 2019;284:84--89.

[7] van Hout MJP, Juffermans JF, Lamb HJ, Kröner ESJ, van den Boogaard PJ, Schalij MJ, et al. Ascending aorta curvature and flow displacement are associated with accelerated aortic growth at long-term follow-up: A MRI study in Marfan and thoracic aortic aneurysm patients. IJC Heart Vasc 2022;38:100926.

[8] Poullis MP, Warwick R, Oo A, Poole RJ. Ascending aortic curvature as an independent risk factor for type A dissection, and ascending aortic aneurysm formation: a mathematical model. Eur J Cardiothorac Surg 2008;33:995--1001.

[9] Renapurkar RD, Setser RM, O'Donnell TP, Egger J, Lieber ML, Desai MY, et al. Aortic volume as an indicator of disease progression in patients with untreated infrarenal abdominal aneurysm. Eur J Radiol 2012;81:e87--93.

[10] Craiem D, El Batti S, Casciaro M, Mousseaux E, Sirieix M-E, Simon A, et al. Age-related changes of thoracic aorta geometry used to predict the risk for acute type B dissection. Int J Cardiol 2017;228:654--660.

[11] Trinh B, Dubin I, Rahman O, Ferreira Botelho MP, Naro N, Carr JC, et al. Aortic Volumetry at Contrast-enhanced MR Angiography: Feasibility as a Sensitive Method for Monitoring Bicuspid Aortic Valve Aortopathy. Invest Radiol 2017;52:216--222.

[12] Sherrah AG, Grieve SM, Jeremy RW, Bannon PG, Vallely MP, Puranik R. MRI in chronic aortic dissection: a systematic review and future directions. Front Cardiovasc Med 2015;2:5.

[13] Dietenbeck T, Craiem D, Rosenbaum D, Giron A, De Cesare A, Bouaou K, et al. 3D aortic morphology and stiffness in MRI using semi-automated cylindrical active surface provides optimized description of the vascular effects of aging and hypertension. Comput Biol Med 2018;103:101--108.

[14] O'Rourke MF, Pauca A, Jiang X-J. Pulse wave analysis. Br J Clin Pharmacol 2001;51:507--522.

[15] Dietenbeck T, Houriez–Gombaud-Saintonge S, Charpentier E, Gencer U, Giron A, Gallo A, et al. Quantitative magnetic resonance imaging measures of three-dimensional aortic morphology in healthy aging and hypertension. J Magn Reson Imaging 2021;53:1471--1483.

[16] Barbosa DC, Dietenbeck T, Schaerer J, D'hooge J, Friboulet D, Bernard O. B-Spline Explicit Active Surfaces: An efficient framework for real-time 3D region-based segmentation. IEEE Trans Image Process 2012;21:241--251.

[17] Erbel R, Aboyans V, Boileau C, Bossone E, Di Bartolomeo R, Eggebrecht H, et al. 2014 ESC Guidelines on the diagnosis and treatment of aortic diseases: Document covering acute and chronic aortic diseases of the thoracic and abdominal aorta of the adult The Task Force for the Diagnosis and Treatment of Aortic Diseases of the European Society of Cardiology (ESC). Eur Heart J 2014;35:2873--2926.

[18] Bullitt E, Gerig G, Pizer SM, Lin W, Aylward SR. Measuring tortuosity of the intracerebral vasculature from MRA images. IEEE Trans Med Imaging 2003;22:1163--1171.

[19] Grisan E, Foracchia M, Ruggeri A. A novel method for the automatic grading of retinal vessel tortuosity. IEEE Trans Med Imaging 2008;27:310--319.

[20] Barat M, Jannot A-S, Dohan A, Soyer P. How to report and compare quantitative variables in a radiology article. Diagn Interv Imaging 2022;103:571--573.

[21] Soyer P, Patlas MN, Bluemke DA. Writing a successful original research paper for a radiology journal. Diagn Interv Imaging 2022;103:285--287.

[22] Davies RR, Gallo A, Coady MA, Tellides G, Botta DM, Burke B, et al. Novel measurement of relative aortic size predicts rupture of thoracic aortic aneurysms. Ann Thorac Surg 2006;81:169–77.

[23] Masri A, Kalahasti V, Svensson LG, Roselli EE, Johnston D, Hammer D, et al. Aortic cross-sectional area/height ratio and outcomes in patients with a trileaflet aortic valve and a dilated aorta. Circulation 2016:1724--1737.

[24] DeLong ER, DeLong DM, Clarke-Pearson D. Comparing the areas under two or more correlated receiver operating characteristic curves: A nonparametric approach. Biometrics 1988;44:837--845.

[25] Elefteriades JA, Mukherjee SK, Mojibian H. Discrepancies in measurement of the thoracic aorta. J Am Coll Cardiol 2020;76:201--217.

[26] Bouaou K, Bargiotas I, Dietenbeck T, Bollache E, Soulat G, Craiem D, et al. Analysis of aortic pressure fields from 4D flow MRI in healthy volunteers: Associations with age and left ventricular remodeling. J Magn Reson Imaging 2019;50:982--993.

[27] Houriez--Gombaud-Saintonge S, Mousseaux E, Bargiotas I, De Cesare A, Dietenbeck T, Bouaou K, et al. Comparison of different methods for the estimation of aortic pulse wave velocity from 4D flow cardiovascular magnetic resonance. J Cardiovasc Magn Reson 2019;21:75.

[28] Soulat G, Scott MB, Pathrose A, Jarvis K, Berhane H, Allen B, et al. 4D flow MRI derived aortic hemodynamics multi-year follow-up in repaired coarctation with bicuspid aortic valve. Diagn Interv Imaging 2022.

[29] Rose MJ, Rigsby CK, Berhane H, Bollache E, Jarvis K, Barker AJ, et al. 4-D flow MRI aortic 3-D hemodynamics and wall shear stress remain stable over short-term follow-up in pediatric and young adult patients with bicuspid aortic valve. Pediatr Radiol 2019;49:57--67.

[30] Guo F, He D, Zhang W, Walton RG. Trends in Prevalence, Awareness, Management, and Control of Hypertension Among United States Adults, 1999 to 2010. J Am Coll Cardiol 2012;60:599--606.

[31] Isselbacher EM, Preventza O, Black JH, Augoustides JG, Beck AW, Bolen MA, et al. 2022 ACC/AHA guideline for the diagnosis and management of aortic disease: A report of the american heart Association/American college of cardiology joint committee on clinical practice guidelines. Circulation 2022;146:e334--e482.

[32] Burman ED, Keegan J, Kilner PJ. Aortic root measurement by cardiovascular magnetic resonance: specification of planes and lines of measurement and corresponding normal values. Circ Cardiovasc Imaging 2008;1:104--113.

[33] Petersen SE, Khanji MY, Plein S, Lancellotti P, Bucciarelli-Ducci C. European Association of Cardiovascular Imaging expert consensus paper: a comprehensive review of cardiovascular magnetic resonance normal values of cardiac chamber size and aortic root in adults and recommendations for grading severity. Eur Heart J - Cardiovasc Imaging 2019;20:1321--1331.

[34] Blanchard C, Lalande A, Sliwa T, Bouchot O, Voisin Y. Automatic evaluation of the Valsalva sinuses from cine-MRI. Magn Reson Mater Phys Biol Med 2011;24:359--370.

[35] Mairesse F, Blanchard C, Boucher A, Sliwa T, Lalande A, Voisin Y. Automatic measurement of the sinus of Valsalva by image analysis. Comput Methods Programs Biomed 2017;148:123--135.

[36] Queirós S, Morais P, Fonseca JC, D'hooge J, Vilaça JL. Semi-automatic aortic valve tract segmentation in 3D cardiac magnetic resonance images using shape-based B-spline explicit active surfaces. SPIE Med. Imaging, vol. 10949, 2019, p. 316--323.

Figures
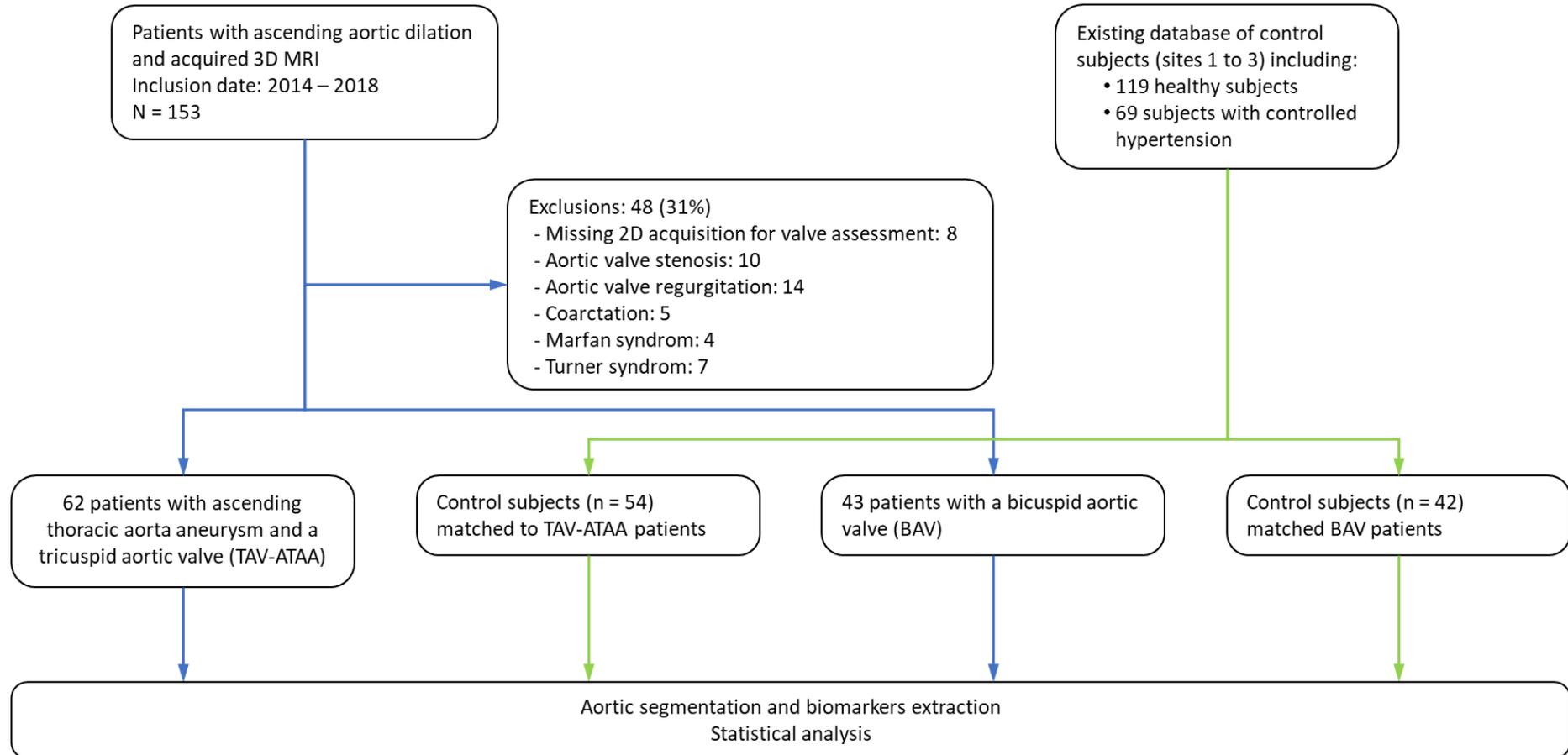
Figure 1 – Study flow chart

Figure 2 - Aortic segmentation and partition into segments

a) Control, b) patient with a tricuspid aortic valve and aneurysm of the thoracic ascending aorta (TAV-ATAA) and c) patient with a bicuspid aortic valve and dilated ascending aorta (BAV). These participants had similar age, height and body surface area: 69 to 71 years, 172 to 183 cm and 1.95 to 2.02 m², respectively. The same scale was used for the 3 participants. Green line: aortic centreline; red: ascending aorta; green: aortic arch; blue: proximal descending thoracic aorta

(a) Control   (b) TAV-ATAA   (c) BAV
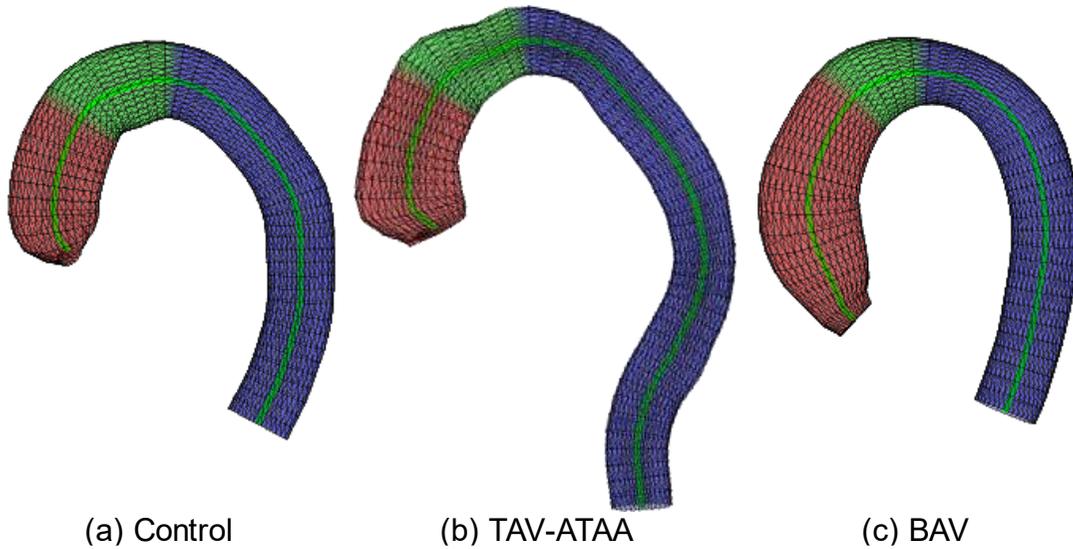
Figure 3 – Aortic morphological parameters of patients with tricuspid aortic valve and ascending thoracic aorta aneurysm (TAV-ATAA)

Boxplot representation of aortic morphological changes between TAV-ATAA patients (red filled boxes) and their matched controls (blue empty boxes) in the ascending aorta (AAo), aortic arch (Arch) and descending aorta (DAo). * $P < 0.05$; ** $P < 0.01$; *** $P < 0.001$. The boxplots show the range (whiskers), interquartile range (box), and median (line within the box).

Figure 4 – Aortic morphological parameters of patients with dilated ascending aorta and bicuspid aortic valve (BAV)

Boxplot representation of aortic morphological changes between BAV patients (red filled boxes) and their matched controls (blue empty boxes) in the ascending aorta (AAo), aortic arch (Arch) and descending aorta (DAo). * $P < 0.05$; ** $P < 0.01$; *** $P < 0.001$. The boxplots show the range (whiskers), interquartile range (box), and median (line within the box).
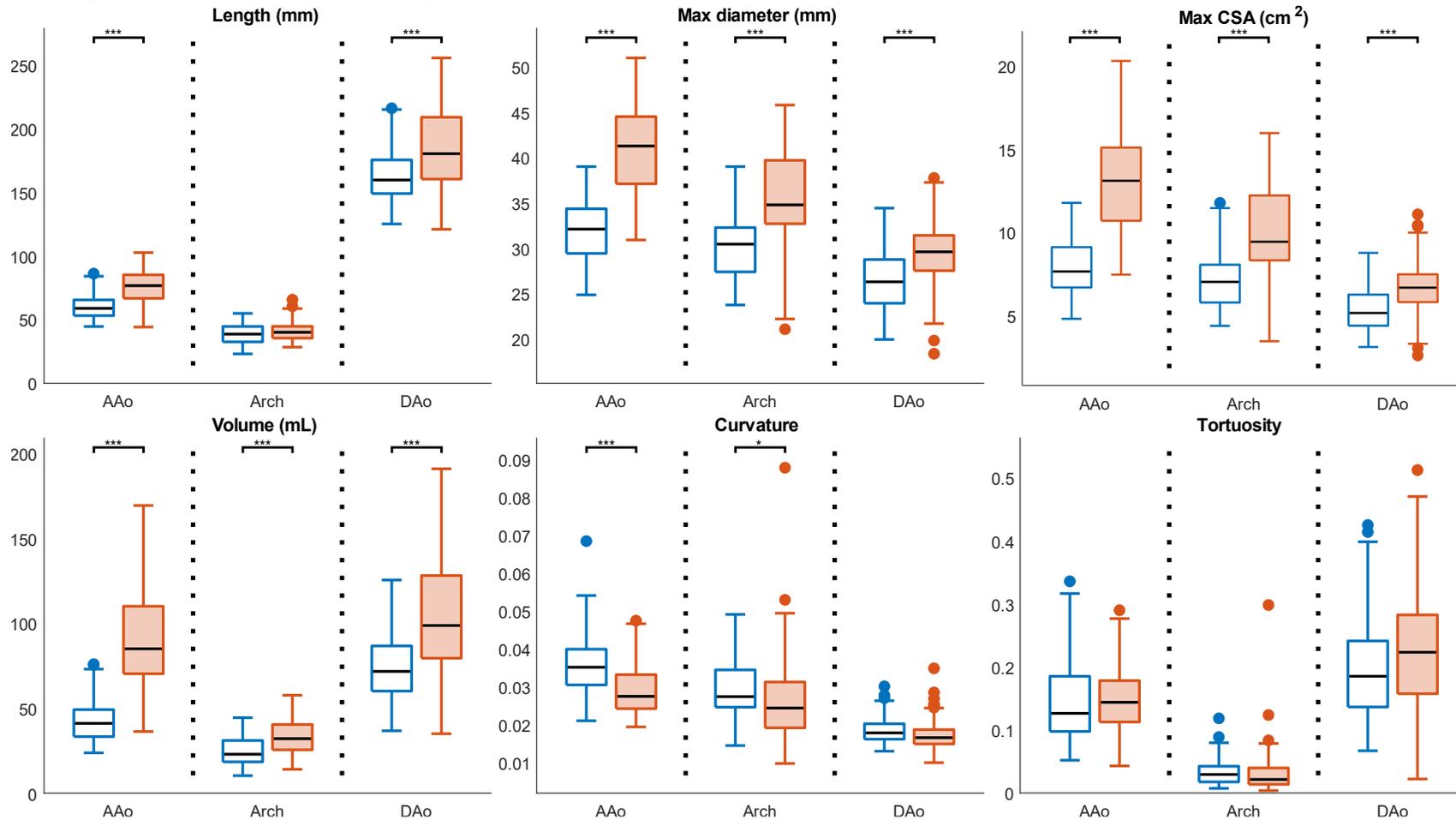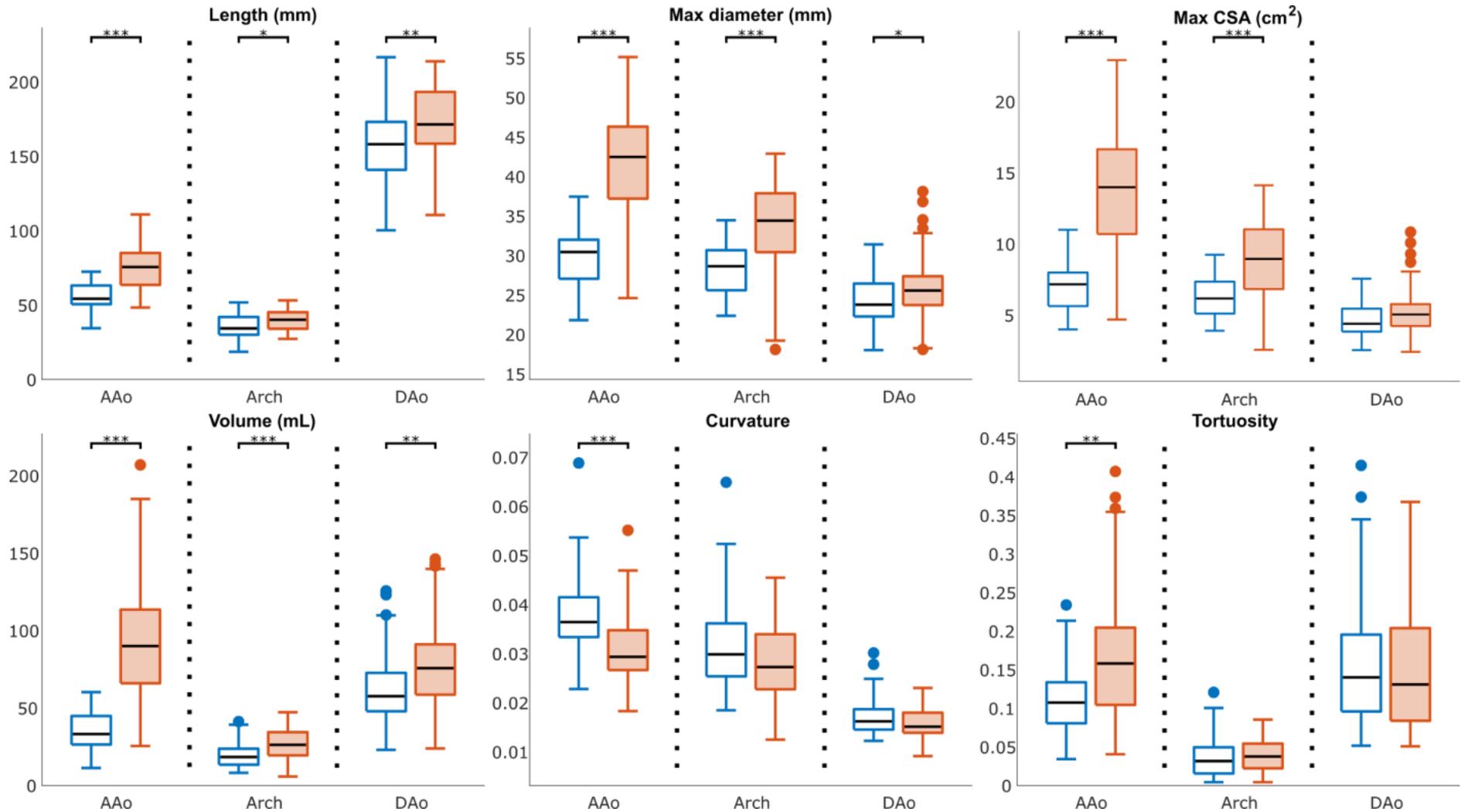
Tables

Table 1 – Participant characteristics

	Controls (Ct)	TAV-ATAA patients	*P*-value	Controls (Cb)	BAV patients	*P*-value
n	54	62		42	43	
Sex (M/F)	39/15	47/15	0.660	34/8	35/8	0.958
Age (years)	68 (59; 73) [33-81]	66 (60; 75) [33-86]	0.886	50 (40; 66) [17-77]	51 (39; 66) [17-76]	0.892
BMI (kg.m^{-2})	24.2 (22.6; 25.9) [18.1-31.8]	25.5 (22.8; 29.1) [17.0-35.9]	0.081	24.1 (21.7; 26.2) [18.1-32.1]	24.4 (21.2; 27.9) [18.0-35.2]	0.539
BSA (m^2)	1.80 (1.72; 1.96) [1.40-2.15]	1.94 (1.73; 2.03) [1.43-2.35]	0.023	1.83 (1.76; 1.98) [1.41-2.15]	1.90 (1.79; 2.02) [1.50-2.38]	0.088
Central SBP (mmHg)	118 (110; 126) [94-144]	125 (115; 138) [98-179]	0.014	114 (108; 121) [86-152]	119 (108; 129) [87-167]	0.176
Central DBP (mmHg)	78 (74; 85) [63-100]	85 (74; 88) [56-105]	0.076	82 (75; 87) [65-101]	80 (75; 89) [53-101]	0.643
Central PP (mmHg)	38 (33; 45) [21-58]	39 (34; 53) [21-89]	0.344	35 (30; 37) [21-51]	34 (29; 43) [20-77]	0.585

Data are median (interquartile range) [min-max].

TAV-ATAA: tricuspid aortic valve-ascending thoracic aorta aneurysm; BAV: dilated ascending aorta and bicuspid aortic valve; Ct: TAV-ATAA controls; Cb: BAV controls; BMI: body mass index; BSA: body surface area; SBP/SDP: systolic/diastolic blood pressure; PP: pulse pressure

Table 2 – Morphological indices of aorta

	Controls (Ct)	TAV-ATAA patients	*P*-value	Controls (Cb)	BAV patients	*P*-value
Ascending aorta						
Length (mm)	59.0 (53.2; 65.7) [44.7-86.3]	76.9 (66.8; 85.7) [44.3-102.9]	< 0.001	54.2 (50.5; 63.3) [34.4-72.4]	75.6 (63.5; 85.0) [48.3-110.1]	< 0.001
Maximal diameter (mm)	32.2 (29.4; 34.5) [24.9-39.1]	41.3 (37.1; 44.6) [31.0-51.1]	< 0.001	30.4 (27.0; 32.2) [21.8-37.4]	42.5 (36.9; 46.5) [24.6-55.1]	< 0.001
Maximal CSA (cm^2)	7.7 (6.7; 9.2) [4.8-11.8]	13.1 (10.7; 15.1) [7.5-20.3]	< 0.001	7.2 (5.6; 8.1) [4.0-11.1]	14.0 (10.6; 16.7) [4.7-22.9]	< 0.001
Volume (mL)	41.1 (33.3; 49.3) [23.7-76.0]	85.0 (70.3; 110.2) [36.3-169.5]	< 0.001	33.1 (26.2; 44.9) [11.3-60.2]	89.9 (65.2; 113.7) [25.4-206.8]	< 0.001
Curvature (mm^{-1})	0.035 (0.030; 0.040) [0.021-0.069]	0.028 (0.024; 0.033) [0.019-0.048]	< 0.001	0.036 (0.033; 0.042) [0.022-0.069]	0.029 (0.027; 0.035) [0.018-0.062]	< 0.001
Tortuosity	0.127 (0.095; 0.187) [0.052-0.336]	0.144 (0.113; 0.179) [0.04-0.29]	0.204	0.107 (0.080; 0.134) [0.034-0.234]	0.158 (0.103; 0.205) [0.04-0.41]	0.001
Aortic arch						
Length (mm)	38.8 (32.5; 44.8) [23.2-55.1]	40.2 (35.5; 44.9) [18.5-65.8]	0.229	34.3 (29.8; 42.0) [18.6-51.8]	40.1 (34.0; 45.3) [27.2-53.1]	0.013
Maximal diameter (mm)	30.5 (27.4; 32.6) [23.8-39.1]	34.8 (32.7; 39.8) [21.1-45.8]	< 0.001	28.6 (25.6; 30.7) [22.3-34.4]	34.4 (30.0; 37.9) [18.1-42.9]	< 0.001
Maximal CSA (cm^2)	7.1 (5.8; 8.1) [4.4-11.8]	9.5 (8.2; 12.3) [3.5-16.0]	< 0.001	6.2 (5.1; 7.4) [3.9-9.2]	8.9 (6.8; 11.1) [2.6-14.1]	< 0.001
Volume (mL)	22.9 (18.3; 31.3) [10.3-44.5]	32.1 (25.2; 40.7) [14.1-57.7]	< 0.001	18.3 (13.3; 23.9) [8.1-41.2]	26.2 (19.4; 34.4) [5.7-47.2]	< 0.001
Curvature (mm^{-1})	0.027 (0.025; 0.034) [0.015-0.049]	0.024 (0.019; 0.032) [0.010-0.088]	0.012	0.030 (0.025; 0.036) [0.013-0.065]	0.027 (0.023; 0.034) [0.013-0.046]	0.091

Tortuosity	0.029 (0.017; 0.044) [0.007-0.119]	0.022 (0.014; 0.040) [0.004-0.299]	0.208	0.032 (0.015; 0.050) [0.004-0.120]	0.037 (0.022; 0.055) [0.004-0.085]	0.349
Descending aorta						
Length (mm)	160 (149; 176) [125-217]	181 (161; 211) [121-256]	< 0.001	158 (140; 173) [100-217]	171 (158; 194) [111-214]	0.010
Maximal diameter (mm)	26.3 (23.9; 28.8) [20.0-34.5]	29.6 (27.5; 31.5) [18.4-37.8]	< 0.001	23.7 (22.2; 26.7) [18.0-31.4]	25.5 (23.6; 27.4) [18.1-38.1]	0.036
Maximal CSA (cm^2)	5.2 (4.4; 6.3) [3.1-8.8]	6.7 (5.8; 7.5) [2.6-11.1]	< 0.001	4.4 (3.8; 5.5) [2.5-7.5]	5.04 (4.12; 5.76) [2.41-10.8]	0.080
Volume (mL)	71.7 (59.7; 87.3) [36.7-125.5]	98.8 (79.1; 129.0) [35.0-191.1]	< 0.001	57.5 (47.5; 73.2) [22.9-125.5]	75.7 (57.6; 92.0) [23.8-146.1]	0.010
Curvature (mm^{-1})	0.018 (0.016; 0.020) [0.013-0.030]	0.017 (0.015; 0.019) [0.010-0.035]	0.051	0.016 (0.015; 0.019) [0.012-0.030]	0.015 (0.014; 0.018) [0.009-0.023]	0.217
Tortuosity	0.185 (0.133; 0.250) [0.067-0.426]	0.224 (0.157; 0.283) [0.022-0.513]	0.089	0.140 (0.095; 0.196) [0.051-0.412]	0.131 (0.083; 0.206) [0.051-0.367]	0.954

Data are median (interquartile range) [min-max].

TAV-ATAA: ascending thoracic aortic aneurysm and tricuspid aortic valve; BAV: dilated ascending aorta and bicuspid aortic valve; Ct: TAV-ATAA controls; Cb: BAV controls; CSA: cross-sectional area

Table 3 – Receiver operating characteristic curve analysis

	AUC	*P*-value	Threshold	Accuracy (%)	Sensitivity (%)	Specificity (%)
Controls (Ct) vs. TAV-ATAA patients						
AAo length indexed to BSA (mm.m^{-2})	0.820 (0.739 - 0.901)	< 0.001	36.4	78.3 (90/115; 70.7 - 85.8)	77.1 (47/61; 66.5 - 87.6)	79.6 (43/54; 68.9 - 90.4)
AAo maximal diameter indexed to BSA (mm.m^{-2})	0.867 (0.795 - 0.939)	0.003	20.6	80.9 (93/115; 73.7 - 88.1)	70.5 (43/61; 59.0 - 81.9)	92.6 (50/54; 85.6 - 99.6)
AAo maximal CSA indexed to BSA (cm^2.m^{-2})	0.900 (0.836 - 0.964)	0.03	7.80	82.6 (95/115; 75.7 - 89.5)	70.5 (43/61; 59.0 - 81.9)	96.3 (52/54; 91.3 - 100)
AAo volume indexed to BSA (mL.m^{-2})	0.935 (0.882 - 0.989)		30.8	88.7 (102/115; 82.9 - 94.5)	88.5 (54/61; 80.5 - 96.5)	88.9 (48/54; 80.5 - 97.3)
Controls (Cb) vs. BAV patients						
AAo length indexed to BSA (mm.m^{-2})	0.827 (0.730 - 0.924)	0.02	33.1	78.3 (65/83; 69.4 - 87.2)	80.5 (33/41; 68.4 - 92.6)	76.2 (32/42; 63.3 - 89.1)
AAo maximal diameter indexed to BSA (mm.m^{-2})	0.876 (0.789 - 0.963)	0.07	20.4	83.1 (69/83; 75.1 - 91.2)	70.7 (29/41; 56.8 - 84.7)	95.2 (40/42; 88.8 - 100)
AAo maximal CSA indexed to BSA (cm^2.m^{-2})	0.900 (0.819 - 0.981)	0.27	7.01	86.8 (72/83; 79.5 - 94.0)	82.9 (34/41; 71.4 - 94.4)	90.5 (38/42; 81.6 - 99.4)
AAo volume indexed to BSA (mL.m^{-2})	0.908 (0.829 - 0.987)		28.5	88.0 (73/83; 80.9 - 95.0)	82.9 (34/41; 71.4 - 94.4)	92.9 (39/42; 85.1 - 100.0)

Ability of 3D MRI aortic morphological measures indexed to body surface area (BSA), to differentiate patients with ascending thoracic aortic aneurysm and a tricuspid aortic valve (TAV-ATAA) or a dilated ascending aorta and a bicuspid valve (BAV) from their matched controls (Ct and Cb, respectively) in terms of receiver operating characteristic (ROC) curve statistics, including area under the ROC curve (AUC), accuracy, sensitivity and specificity as well as abnormality threshold. AAo: ascending aorta.

Sensitivity, specificity and accuracy are reported as percentages, numbers in parentheses are corresponding proportions followed by 95%

confidence intervals. *P*-values are computed for comparison against AAo volume indexed to BSA using a DeLong test.